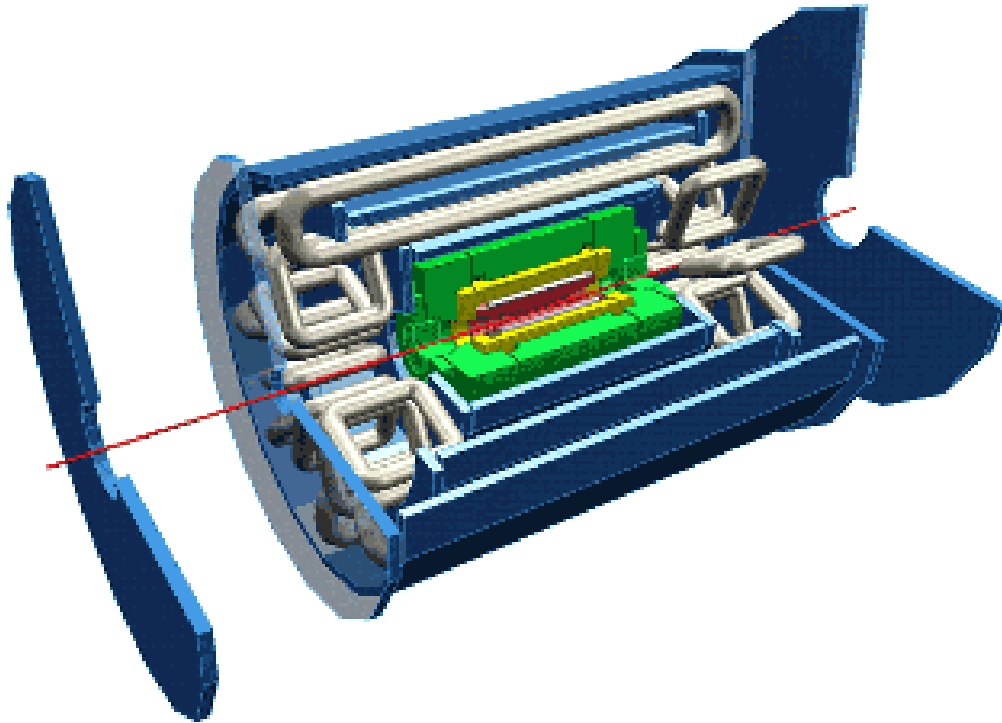


Background Analysis of Simulated ATLAS Events in the Higgs Boson to Two Photon Decay Channel

Undergraduate Thesis

Robert Nordsell



**Southern Methodist University
Dallas, Texas**

April 28, 2005

Table of Contents

LIST OF FIGURES	ii
INTRODUCTION	1
THE ATLAS EXPERIMENT	7
RESEARCH CONDUCTED	11
Photons	12
Electrons	13
Particle Jets	15
Muons	16
Bjets	17
Tau Jets	18
COMPARISONS OF TRUTH AND RECONSTRUCTED PARTICLES	20
Photons	20
Electrons	21
Particle Jets	22
Muons	24
Tau Jets	25
MISSING TRANSVERSE MOMENTUM	26
MASS OF THE HIGGS BOSON	28
TOTAL ENERGY OF PARTICLE JETS FOR EACH EVENT	30
CONCLUSION	31
REFERENCES	

List of Figures

Figure	Page
1. Standard Model	2
2. Pion Decay	4
3. ATLAS Detector Components	8
4. ATLAS Profile	10
5. Photon Histograms	13
6. Electron Histograms	14
7. Particle Jet Histograms	16
8. Muon Histograms	17
9. Bjet Histograms	18
10. Tau Jet Histograms	19
11. Truth and Reconstructed Photons	21
12. Truth and Reconstructed Electrons	23
13. Truth and Reconstructed Particle Jets	24
14. Truth and Reconstructed Muons	26
15. Truth and Reconstructed Tau Jets	27
16. Missing Transverse Momentum	28
17. Mass of Higgs Boson	29
18. Particle Jet Total Energy	31

Introduction

It is obvious that most things in our macroscopic world are not pure substances, but rather contain an array of more basic and fundamental constituents. A cake, for example, is made of flour, sugar, and other ingredients. The human body is a system of organs, comprised of tissue, which is composed of cells. These observations beg the question, what is the most basic structure of matter? The study of particle physics is motivated by answering this question.

It was only 100 years ago that the smallest constituent of matter was thought to be the atom. The concept of the atom was originated around 440 BC by Leucippus of Miletus and his pupil Democritus. Democritus reasoned that if matter could be infinitely divided, it could also be completely disintegrated and never put back together. Thus he used the Greek word atomos, meaning indivisible, to describe this concept, essentially stating that every massive object contains an integral number of atoms. While the idea of atoms was discussed by later Greek philosophers, the notion of atomos was eventually abandoned, and matter was largely thought to be continuous until the modern era.

It was in the nineteenth century that the atomic theory revolutionized science, and as experiments began in chemistry, and later physics, to search for elementary particles, the concept of continuous matter had been abjured. In the first quarter of the twentieth century, Ernest Rutherford discovered that the atom was comprised of a positively charged nucleus surrounded by orbiting electrons. In 1932 James Chadwick discovered the neutron, showing that the nucleus consisted of more than just positively charged protons. The third quarter of the twentieth century brought about the finding that protons and neutrons consisted of even smaller entities called quarks.

From this plethora of particles discovered inside a period of 100 years the Standard Model of Fundamental Particles and Interactions was created (figure 1).

Leptons		Quarks	
Spin = 1/2		Spin = 1/2	
Charge = 1	Charge = 0	Charge = 2/3	Charge = -1/3
Electron, e	Electron Neutrino, ν_e	Up, u	Down, d
Muon, μ	Muon Neutrino, ν_μ	Charm, c	Strange, s
Tau, τ	Tau Neutrino, ν_τ	Top, t	Bottom, b

Gauge Bosons	charge
spin = 1	
Photon, γ	0
W^+	+1
W^-	-1
Z^0	0
Gluon, g	0

Figure 1 – The Standard Model of Particle Physics

The Standard Model is divided up into two main categories of fermionic and bosonic particles. Fermionic particles are particles that have a half-integer spin, while bosonic particles have integer spin. The fermions in the standard model include the quarks and the leptons, the standard model bosons include the photon, gluon, and W and Z bosons. These particles, as far as we empirically know, are the most fundamental particles in the universe, and can be considered as point particles for all intents and purposes.

Leptons are spin $\frac{1}{2}$ particles that are weakly interacting. They are organized first in columns by their charge, and then in rows by their mass (see figure 1). Thus, the electron and its associated neutrino are the least massive leptons (and therefore the most stable) for their respective charges, while the tau and its associated neutrino are the most massive. As stated earlier leptons interact weakly and exchange W^\pm , or Z^0 bosons when interactions occur.

The other family of fermionic particles in the Standard Model consists of quarks. Quarks are spin $\frac{1}{2}$ particles that interact both weakly and strongly (via interactions by the exchange of gluons) as well as electromagnetically. Quarks are the fundamental constituents of a class of particle called hadrons, which contains two subclasses called baryons and mesons. Baryons, such as protons and neutrons, are fermionic hadrons containing three quarks with half-integer spin. There are about 120 different types of baryons. Mesons, on the other hand, are bosons (defining them as integer spin particles) that contain a quark-antiquark pair. There are about 140 types of mesons.

The final class of particles in the Standard Model is called gauge bosons. These are the particles which mediate the fundamental physical forces. Weakly interacting particles, such as quarks and leptons, will exchange W^\pm , or Z^0 bosons, which have charges of ± 1 and zero, respectively. Gluons are the mediators of the strong force. These particles have no mass, no charge, and are responsible for interactions between quarks and all hadrons. Similar to gluons, photons also have no mass and no charge, but photon interaction is only experienced by charged particles.

The heavier elementary particles may decay to lighter ones. For example, a π^+ (u and d quark combination) can decay via the weak interaction, W^+ , into a μ^+ and ν_μ . This

decay is allowed because the pion has a larger mass than the muon and the neutrino combined. Feynman diagrams are used to describe these processes visually, and the π^+ decay just described is shown in figure 2. Within these decay and collision interactions, however, conservation laws such as energy, mass, and charge must apply, such that not all possible combinations of particle interactions are allowed.



Figure 2 - π^+ decay into μ^+ and ν_{μ} . The flow of time points upward in this diagram.

While the Standard Model is an organized representation of the particles we have currently observed, there are many other theories such as supersymmetric particles and the Higgs boson, which have not yet been experimentally observed. The current generation of particle physics experiments, scheduled to begin in 2007, will allow us to observe supersymmetric particles and the Higgs boson, if they exist within certain mass limits.

The theory of supersymmetry (SUSY) would effectively double the size of the Standard Model. In SUSY, every fermionic particle has a corresponding bosonic counterpart, and every bosonic particle has a similar fermionic counterpart. The name of these theoretical particles corresponds to the name of its counterpart with an 's' added to the beginning for the supersymmetric bosons, and the name of its counterpart with 'ino' added to the end for the supersymmetric fermions. For example, the electron's SUSY partner is called the selectron, while the W boson's SUSY partner is the Wino.

The Higgs boson is a theoretical particle that interacts directly with all massive fermionic and bosonic particles. Similar to the exchange of photons between charged particles, the exchange of the Higgs particle between all other particles generates a field and the interaction with this field gives the particles their masses.

Given such a complicated theory, one could easily ask how it is that we know such particles even exist, and how are their properties measured when we find them? Microscopes certainly do not allow us to peer into the realm of the atomic, much less subatomic, so how do we begin to identify and classify particles that we can not physically observe using our five senses? The answer lies in quantum mechanics, which states that the shorter wavelengths needed to probe the smallest distance scales require higher and higher energies according to the energy equation $E = hc/\lambda$, where h is Planck's constant, c is the speed of light, and λ is the wavelength. Thus experimental particle physics, which attempts to empirically verify the theories of the smallest constituents of matter, requires the highest energy probes available. The particles which make up this high energy probe must also obey energy, mass, and momentum conservation laws such that, $E^2 = p^2c^2 + (mc^2)^2$, where E is the energy, p is the particle's momentum, m is its mass, and c is the speed of light.

The largest energies and momenta for probing the physics of the smallest distance scales are made available through high energy collisions of charged particles. These collisions take place in very large scale devices called accelerators. The two types of accelerators are called linear and circular accelerators. After the collisions take place, detectors are set up symmetrically around the point of collision to track and identify particles.

High-energy accelerators, in general, use protons or electrons (or their respective antiparticles) in collisions. These particles are used for two reasons. First, protons and electrons are both stable and commonly occurring charged particles. Second, a wide variety of elementary particles can be created and observed from these collisions. This now raises the question of how electrons and protons are accelerated in linear and circular detectors. Both types of accelerators use the electromagnetic fields to accelerate and direct a charged particle at a target, but use slightly different methods.

The linear accelerator accelerates particles in a straight line directed at either a fixed target or at a colliding beam. Parallel plates laid perpendicularly to the beam line are supplied with a potential difference such that the electric field is pointing in the appropriate direction to accelerate the particles based on their charge. The particles pass through holes in a successive series of parallel plates in such a way that as the particles pass through one plate, the polarity of the plate immediately shifts to “push” the particles away from that plate toward the next. As the particles approach the speed of light, the frequency at which the plates switch polarity becomes that of microwave frequencies. Thus, at higher speeds microwave cavities are used in place of the parallel plates. Unfortunately these higher energies require exceptionally long accelerators, which lead to higher costs and more space. The Stanford Linear Accelerator, for example, is two miles long.

Circular accelerators operate under the same electromagnetic principles as linear accelerators. However, circular accelerators use magnetic fields in conjunction with parallel plates to bend the path of the particle, as well as to focus the particles. The benefit to a circular over a linear accelerator is that the particles can be accelerated

through the same parallel plates as many times as needed to accelerate the particles to the desired energies. However, the drawback is that as the charged particle beams are bent through the magnetic fields they emit electromagnetic radiation, called synchrotron radiation. Because the particles are constantly radiating energy, more power needs to be supplied to the electric fields. Because the power lost in synchrotron radiation is proportional to the inverse of the mass to the fourth power, this is not a serious problem for heavier particles like protons, but it is impractical to accelerate electrons through higher energies than 100 GeV. The accelerators which operate at the highest energies are circular and use protons (or antiprotons) in their collisions. These include the Tevatron at Fermilab in Illinois, and beginning in 2007, the LHC (Large Hadron Collider) at the CERN laboratory in Geneva, Switzerland.

The ATLAS Experiment

ATLAS (A Torodial LHC ApparatuS) is one of 4 experiments at the LHC which is designed to detect high energy proton-proton collisions that will hopefully yield a glimpse of supersymmetric particles and the Higgs boson. ATLAS is the largest experiment at the LHC, and the international collaboration for ATLAS includes nearly 2,000 scientists from 34 different countries.

The LHC at CERN is the largest circular accelerator in the world with a circumference of 16.6 miles. The reason that it is necessary to construct such a large circular accelerator is because with a larger radius of curvature the magnetic fields required to bend the beam and keep it in its proper orbit become lower, and thus higher energies can be achieved for a given strength of magnet. Instead of accelerating protons to their maximum energies and then allowing them to hit a stationary target as in a fixed

target experiment, the LHC accelerates two proton beams and collides them with each other. This produces energy in the collision that is twice the amount that is used in accelerating each beam. At the LHC the energy of each proton beam is 7 TeV, producing a collision energy of 14 TeV between the two beams.

When the proton beams collide, an array of particles will be produced from the collision sending them in all directions. The challenge of the experiment is to track, detect, and identify these particles. To do this, ATLAS is comprised of a complex system of detectors symmetrically arranged around the beam axis in a way that most efficiently identifies and tracks particle signatures. Figure 3 shown below provides an illustration of the ATLAS detector.

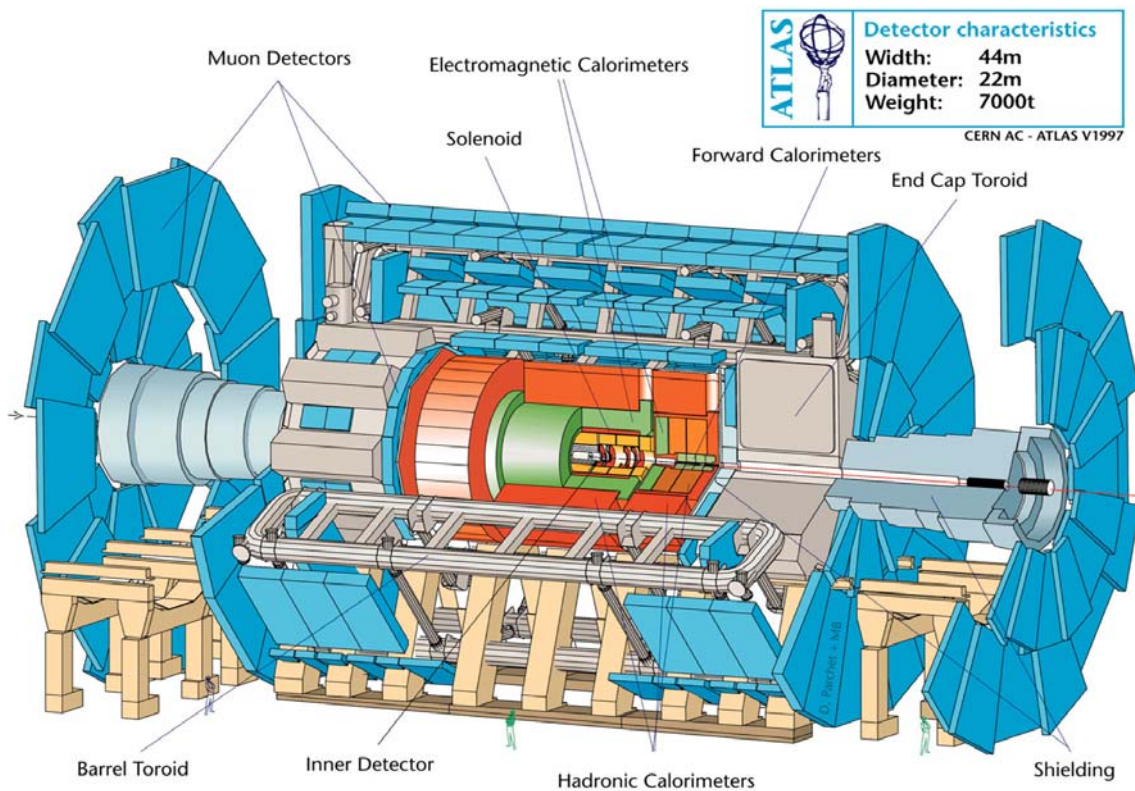


Figure 3 – Components of the ATLAS detector

The inner detector tracks the paths of electrically charged particles. The tracker's innermost sensors are semiconductor devices surrounded by thousands of straws with wires through their axes. High voltages are applied to these wires, which are filled with gas, and when a charged particle travels through the straw the gas is ionized. When these ions reach either wire or the outside of the straw, the resulting electrical pulses are recorded. The inner detector sits in a strong magnetic field so that the trajectories of the charged particles will bend, and the momentum, direction, and charge can be recorded and processed.

Surrounding the inner tracker are the calorimeters. These calorimeters are capable of measuring the energies of charged and neutral particles. Metal plates serve as absorbers for the energy from the particles, and when the particles collide on the absorbers a shower of particles is created, which is detected by the sensing elements. The sensing element in the inner sections of the calorimeters is liquid argon. When the particles from the shower created by the absorbers collide with the liquid argon electrons are liberated, and their electrical signals are recorded. The outer sections of the calorimeters are made of scintillating plastic that liberates photons when struck by the shower of particles. The light (photons) emitted from the scintillator is also processed and recorded.

The outermost part of the detector is the muon spectrometer. Muons are the only charged particles that can traverse the inner detector and the calorimeters and reach the outer part of the detector. The muon spectrometer detects muons through thousands of sensors, similar to those of the inner detector, placed in a magnetic field produced by

large superconducting toroids. The trajectory of the muon is tracked, thus enabling us to determine the momenta of the muons.

Symmetry is very important in experimental particle physics because it makes particle identification calculations much simpler. The ATLAS detector is built with cylindrical symmetry. The proton beams form the z-axis, and special orientation around the z-axis is defined by phi (ϕ) and eta (η). Phi is the azimuthal angle around the beam axis. The pseudorapidity eta is a function of the polar angle theta (θ) which is given by the formula $\eta = \ln(\tan(\theta/2))$. Figure 4 shows the first quadrant of the detector with cones of equal eta shown by the dashed diagonal lines. The electromagnetic (EM) calorimeter in the barrel spans a volume between eta of 0 to ± 1.5 , while the inner and outer end caps of the EM calorimeter cover eta between ± 1.5 and ± 3.2 . The forward calorimeter is designed to detect particles with eta between ± 3.2 and ± 4.9 . Transitions between detector elements occur where eta equals ± 1.5 and $\pm(3.2 - 3.5)$. These are the angles at which the barrel and end cap EM calorimeters meet and where the end cap EM calorimeters meet the forward calorimeter, and these intersections contain cracks in which the particles can slip through undetected.

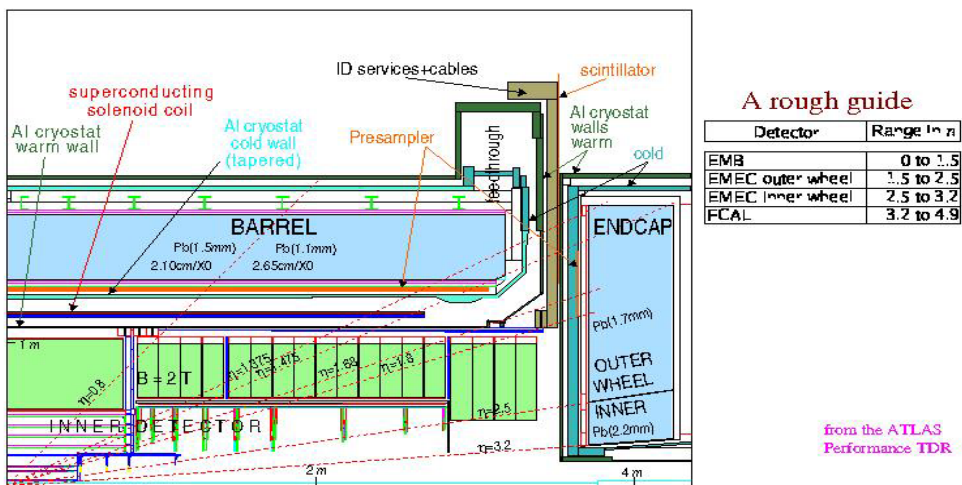


Figure 4 – Profile of the ATLAS detector

Once particles are detected in the various trackers and calorimeters, their signals are sent to a series of triggers. The triggers are used to sort out events which will be investigated further from background events which will be thrown away. The signals from the events which pass through the triggers are then collected by the Data Acquisition System (DAQ), and these are recorded, processed, and made available to physicists for study.

Before the experiment can begin, studies are performed to ensure that this system of recording and processing data is working properly. This is done by what is known as Monte Carlo simulation, which is a computer simulation of the entire process from the collision of the proton all the way to the processing of the data signal. This process is done in several stages. First, the collision of the two protons and their fragmentation into other particles is simulated by a program called an event generator. Then the interaction of the particles with the detector is simulated by a program called Geant. The output of Geant is then digitized so that it is in the same format as the output of the DAQ. Then this data is passed through the ATLAS data reconstruction program, called Athena. Once the signals have been reconstructed, they can then be investigated to see if the whole system is working properly.

Research Conducted

The portion of the ATLAS experiment that I have studied with David Joffe and Ryszard Stroynowski is Monte Carlo simulations of proton-proton collisions that produce a Higgs boson, which decays into two photons. Our main concentration in this experiment was studying the background particles that are produced from the proton-proton collisions. We would like to get an understanding of the vast number of particles

that we can expect to see when the experiment goes online in 2007, including photons, electrons, particle jets, muons, bjets, and tau jets.

Our study consisted of a particular simulation in which we generated a sample of 10,000 events, all of which produced a Higgs boson that decayed into two photons. Of these events 5,470 passed the reconstruction cuts, which required the presence of at least one photon with 10 GeV of transverse momentum. For each type of particle which can be identified in the ATLAS detector, we analyzed the number of particles that were generated for all of the events, their eta and phi distributions, their energies, and their transverse momenta. All of the events were reconstructed both in Athena version 9.0.1 and version 10.0.0. In the following explanations of the background particles studied, only the results from Athena 10.0.0 will be discussed because the efficiency of reconstruction had been improved between the two versions.

Photons

The histograms below detail the reconstruction and identification of photons for the 5,470 final events. The nparticle histogram (number of particles) shows that most of the events consisted of two and only two photons, which is what we would expect since the condition placed on the simulation was that the Higgs would decay into two photons. We observe additional photons due to the decay of other particles that yield a photon, or misidentification of other particles as photons, and we see only one photon when photons slip through the cracks between the barrel and the end caps. The eta and phi distributions show that photons are peaked in the central portion of the detector and are evenly distributed azimuthally. The energy and transverse momentum (pt) graphs display peaks around 60 GeV, which is an expected result because we know that the mass of the Higgs

particle is around 120 GeV, and we know that at least two photons from Higgs decays were created in every event. Energy conservation tells us that if the Higgs particle decays into two photons, the invariant mass of the photons must equal the mass of the Higgs.

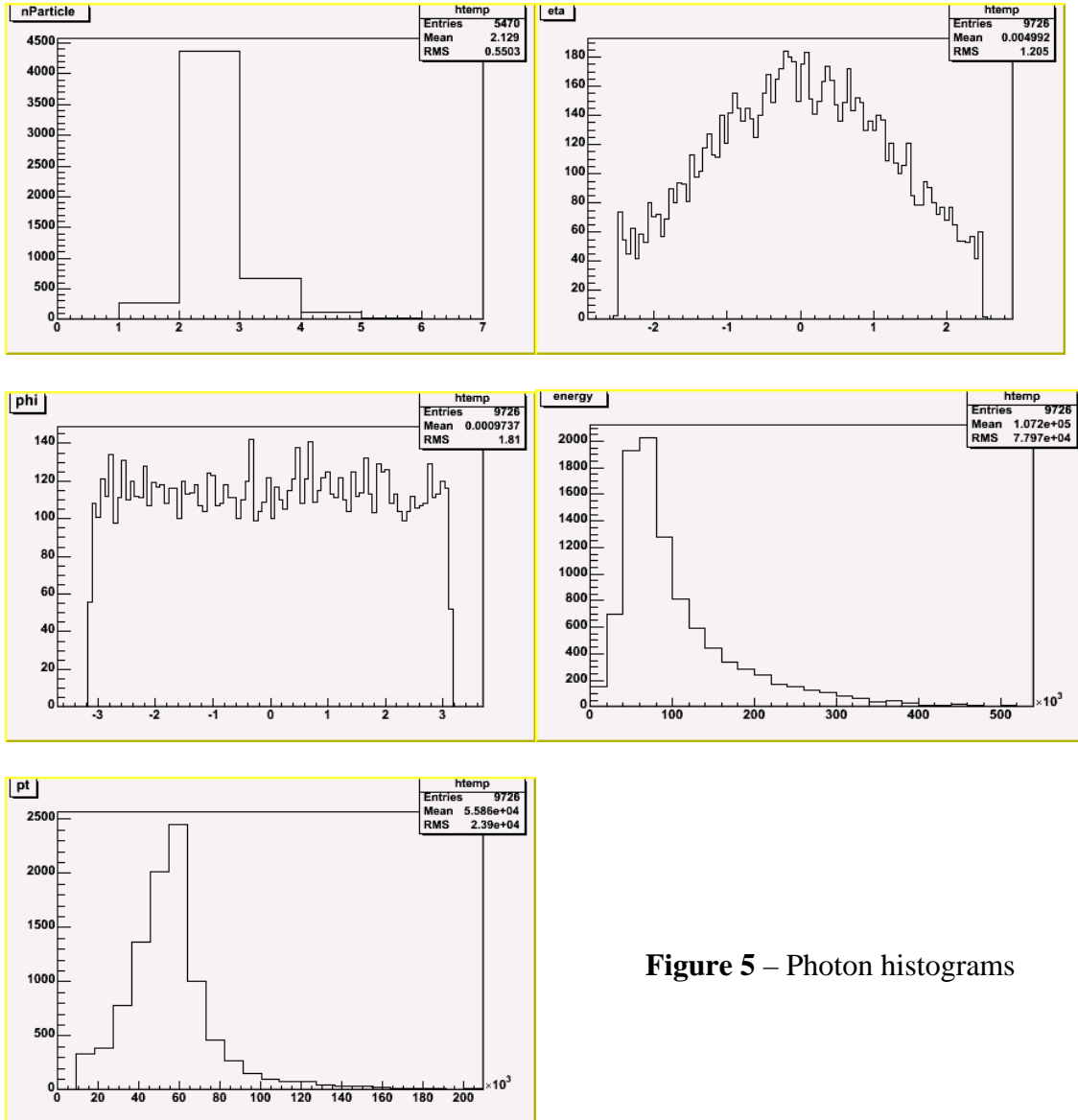


Figure 5 – Photon histograms

Electrons

In most of the collisions only one electron was produced. The eta and phi histograms do not have profiles which are as smooth as the distributions for photons

because the statistics are much smaller. However, some details are still visible; where η equals ± 1.5 there are dips in the graph, which shows where electrons slipped through the cracks between the barrel and the end caps. The energy and pt plots are what we would expect, in that the number of electrons decreases as energy and pt increases, except that instead of a consistent downsloping pt curve there is a spike near 60 GeV. This leads us to hypothesize that photons may be misidentified as electrons.

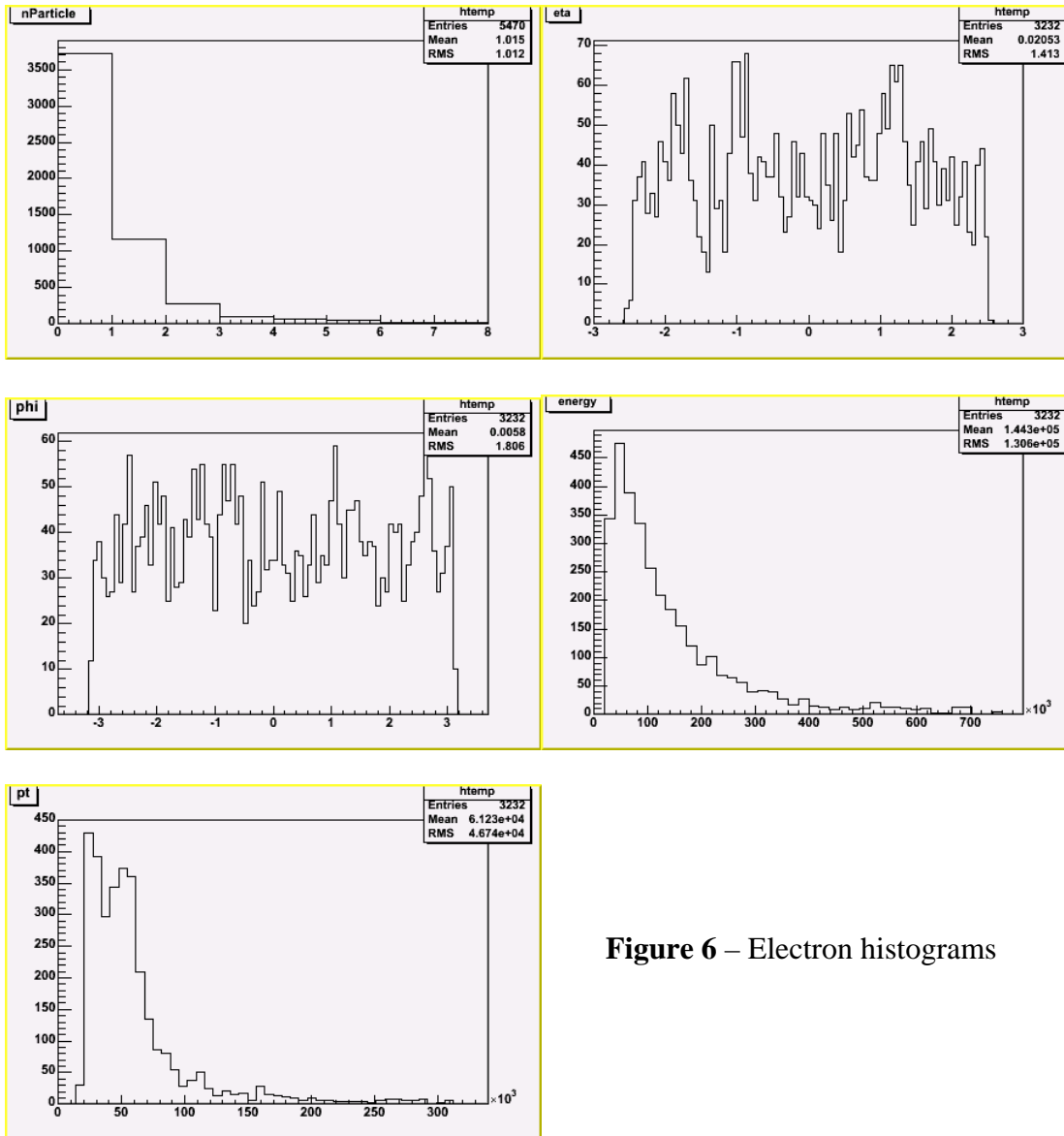


Figure 6 – Electron histograms

Particle Jets

The greatest number of particles detected in each event fall under the category called particle jets. These jets are generally the end result of quarks and gluons which emerge from the proton-proton collision. Because these particles have a color charge in the strong force, they can not remain free particles and quickly polarize the vacuum around them to produce larger structures, hadrons and mesons, which are color neutral. The collection of hadrons and mesons which are produced by each quark or gluon is known as a 'jet'.

As particle jets are essentially showers of particles and their paths can be traced back to where the particles originally branched out from, there will be many particles combined together to form each jet and these are detected in both the hadronic and the electromagnetic calorimeters. Each event generates approximately nine particle jets which are evenly distributed azimuthally about the beam axis. The eta distribution shows that the particle jets are peaked in the central region of the detector, and slip through the cracks where eta approximately equals ± 1.5 and ± 3.5 . As with the electrons, we see a pattern of the number of particle jets tapering off as energy and p_t increase. However, as in the case of the electrons, there is a bump near 60 GeV, which leads us to the conclusion that photons are also being counted as particle jets.

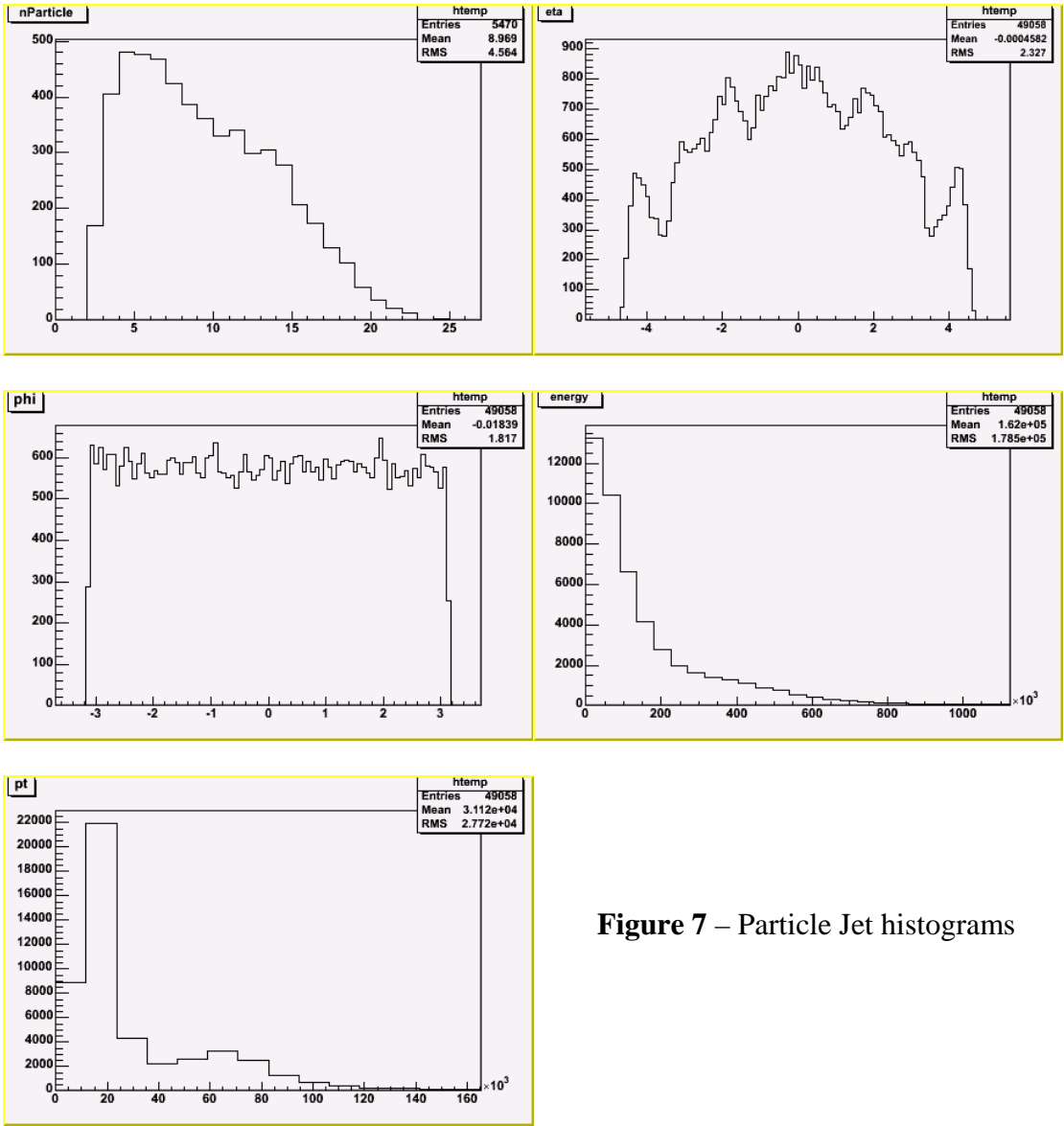


Figure 7 – Particle Jet histograms

Muons

The most abundant particles produced in proton collisions are pions, and as charged pions decay into muons, we can expect that many of the events will contain muons, and that is indeed the case. There were a total of 22,336 muons identified in our 5,470 event sample. Like photons, electrons, and particle jets, muons are distributed azimuthally about the beam axis. Eta, however, takes on a different distribution than every other particle, inasmuch as relatively few muons are detected near the central

region of the detector. Rather, muons are mostly detected where eta is greater than ± 2.0 . We believe that muons are most detected often detected in the forward regions of the detector because the pions from which they are produced are peaked in the forward direction, and the length from the collision point to the muon spectrometer in the central region does not allow as much time for muon decay.

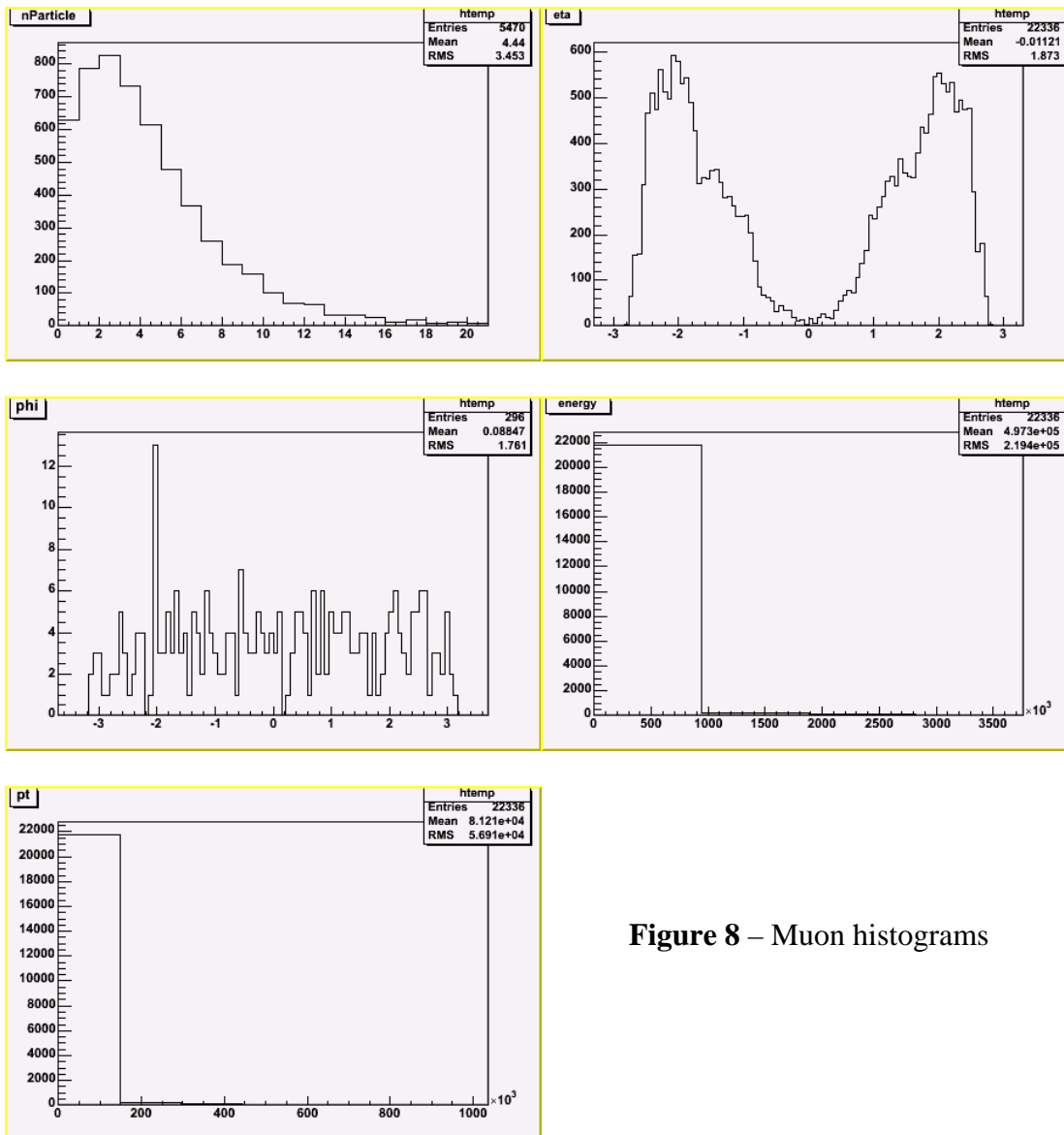


Figure 8 – Muon histograms

Bjets

Bjets are particle showers resulting from the decay of bottom quarks, which produce other particles. Identification of bjets involves being able to reconstruct particle shower tracks back to the origin of dispersion, to determine whether or not the origin, or vertex, of the jet, was displaced from the point of the proton-proton collision. Only 3,369 jets identified as bjets were recorded, and consequently the eta and phi distributions are not smooth. However, as with other particle classes, it can be observed that bjets are azimuthally symmetric and dips in eta are beginning to form near $\eta = \pm 1.5$. As expected, we see a peak in the energy and pt histograms and then the number of bjets declines as energy increases.

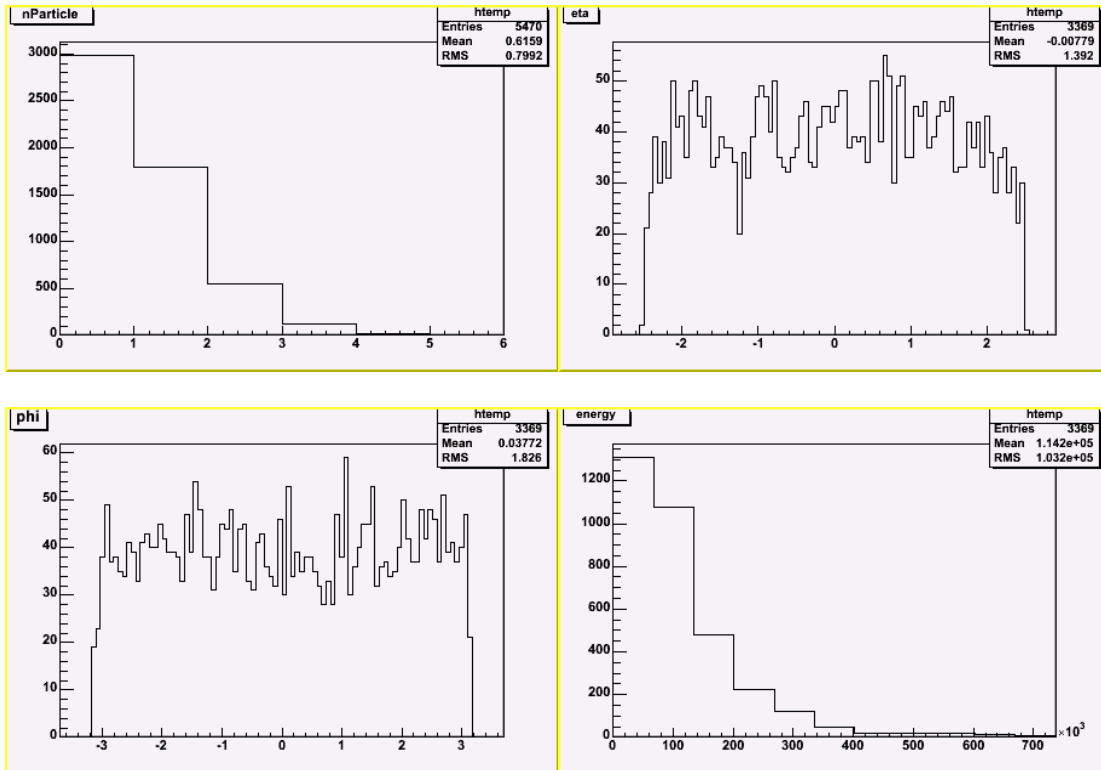


Figure 9 – Bjet histograms

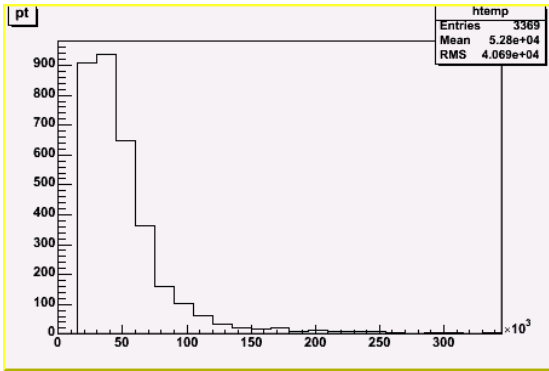


Figure 9 cont. – Bjet histograms

Tau Jets

Tau jets are much like bjets except that the origin of the particle shower is the tau. Tau jets are identified by the small angle cone of the particles in the jet. Nearly 5,000 of the events recorded no tau jets. Because of the sparse number of tau jets, the eta and phi distributions have no discernable resolution, but we can assume that at least phi would be azimuthally symmetric with more events. Tau jet energy and pt peak and then go to zero as energy increases. However, an area of concern is the hump around 55 GeV in the pt histogram, suggesting that photons are being misidentified as tau jets.

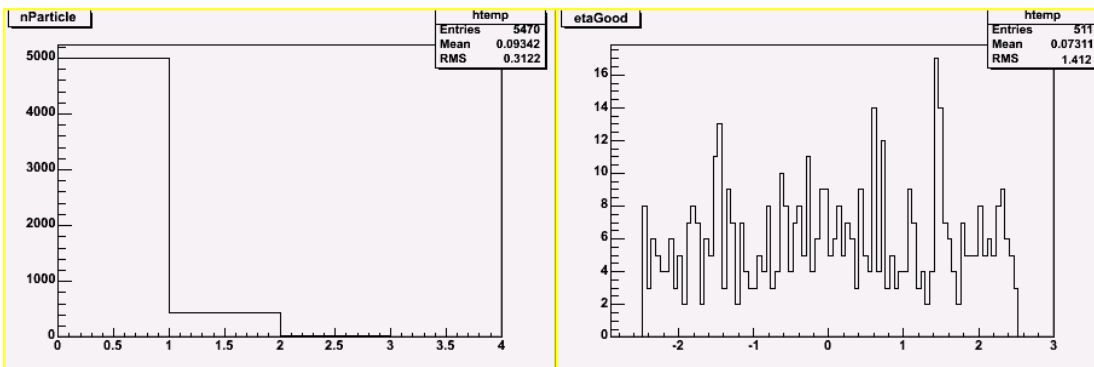


Figure 10 – Tau Jet histograms

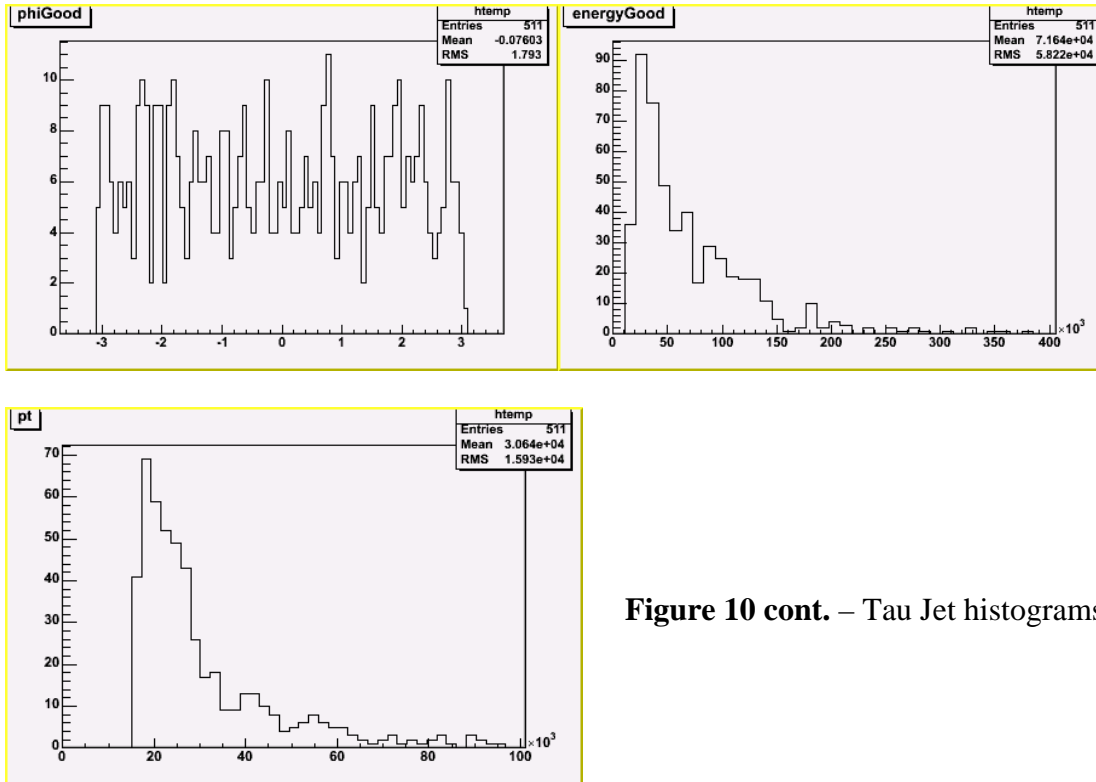


Figure 10 cont. – Tau Jet histograms

Comparisons of Truth and Reconstructed Particles

Up until this point, we have only analyzed particles that had been reconstructed in Athena version 10.0.0. It is imperative that we now make comparisons between the original particles created in the event generator and the reconstructed particles to exploit inefficiencies and potential programming errors in Athena. All the particles from the event generator simulation of the proton-proton collision and the Higgs decay are collected in a separate part of the software known as the ‘truth’. A small sample of the particles from the Geant simulator is also included in the truth. The energy and angle distributions of the truth particles can then be compared with the reconstructed distributions.

Photons

The biggest difference between the truth and reconstructed photon distributions is that there are approximately 4,800 more truth photons, which leads us to believe that some photons are being lost in the reconstruction process. Notice that there are never fewer than two truth photons generated due to the condition that the Higgs will decay into two photons. The eta and pt distributions for the truth and reconstructed photons are nearly identical (with the exception of the difference in the number of particles).

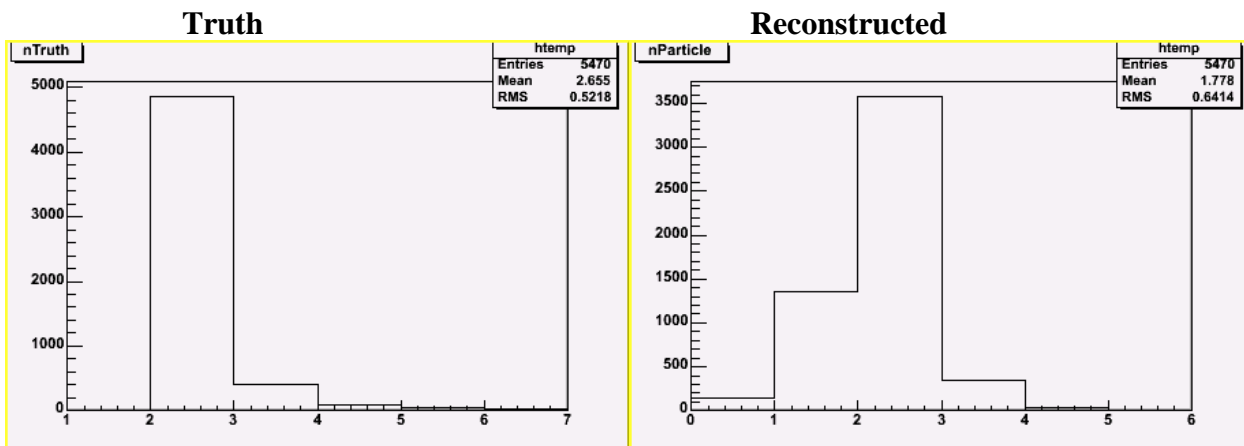


Figure 11 – Truth and reconstructed photon histograms

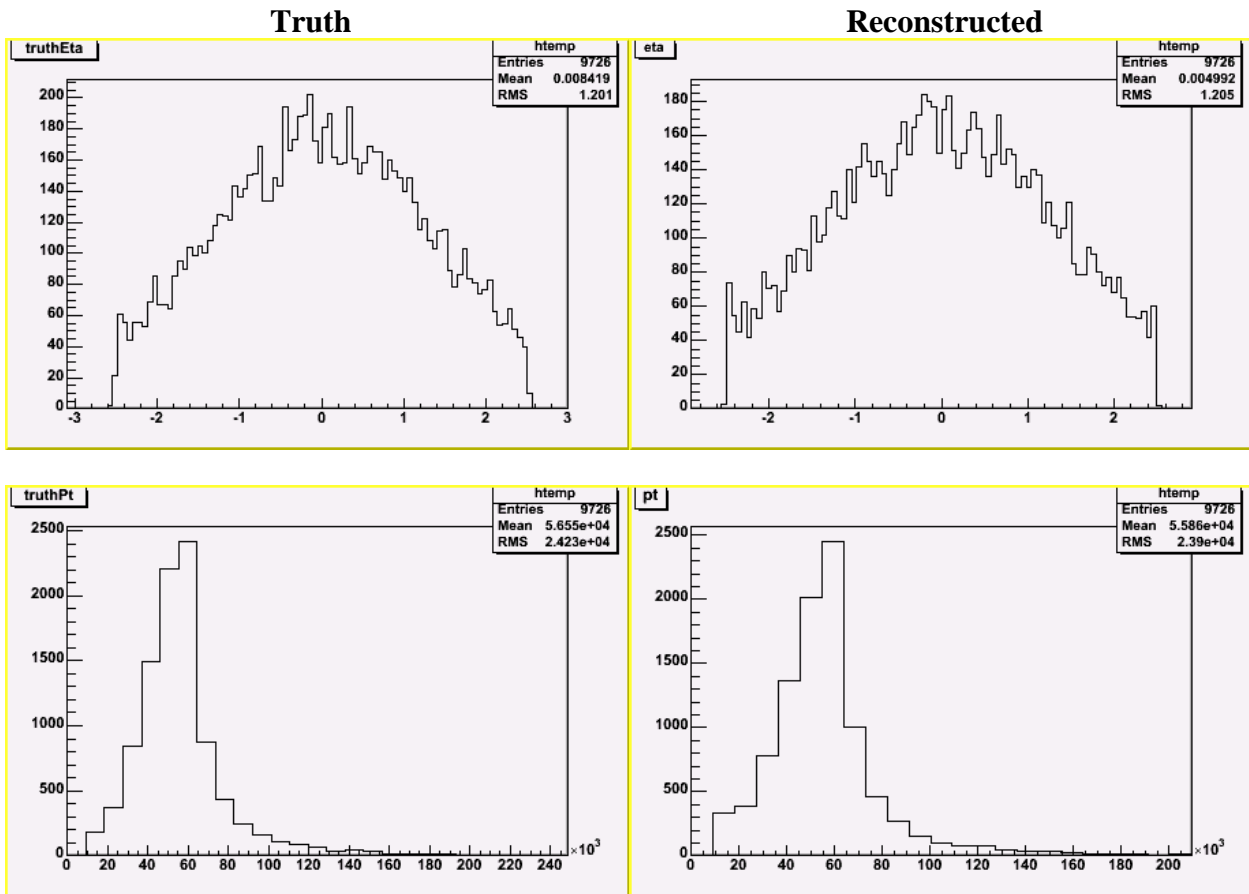


Figure 11 cont. – Truth and reconstructed photon histograms

Electrons

There were significantly fewer truth electrons than reconstructed electrons, with only 79 truth electrons and a much higher 3,232 reconstructed electrons. We believe that this enormous difference in electrons is due to photons being misidentified as electrons. Evidence for this hypothesis is the spike between 40 and 60 GeV, which roughly corresponds to the energy of one photon created by the decay of the Higgs particle.

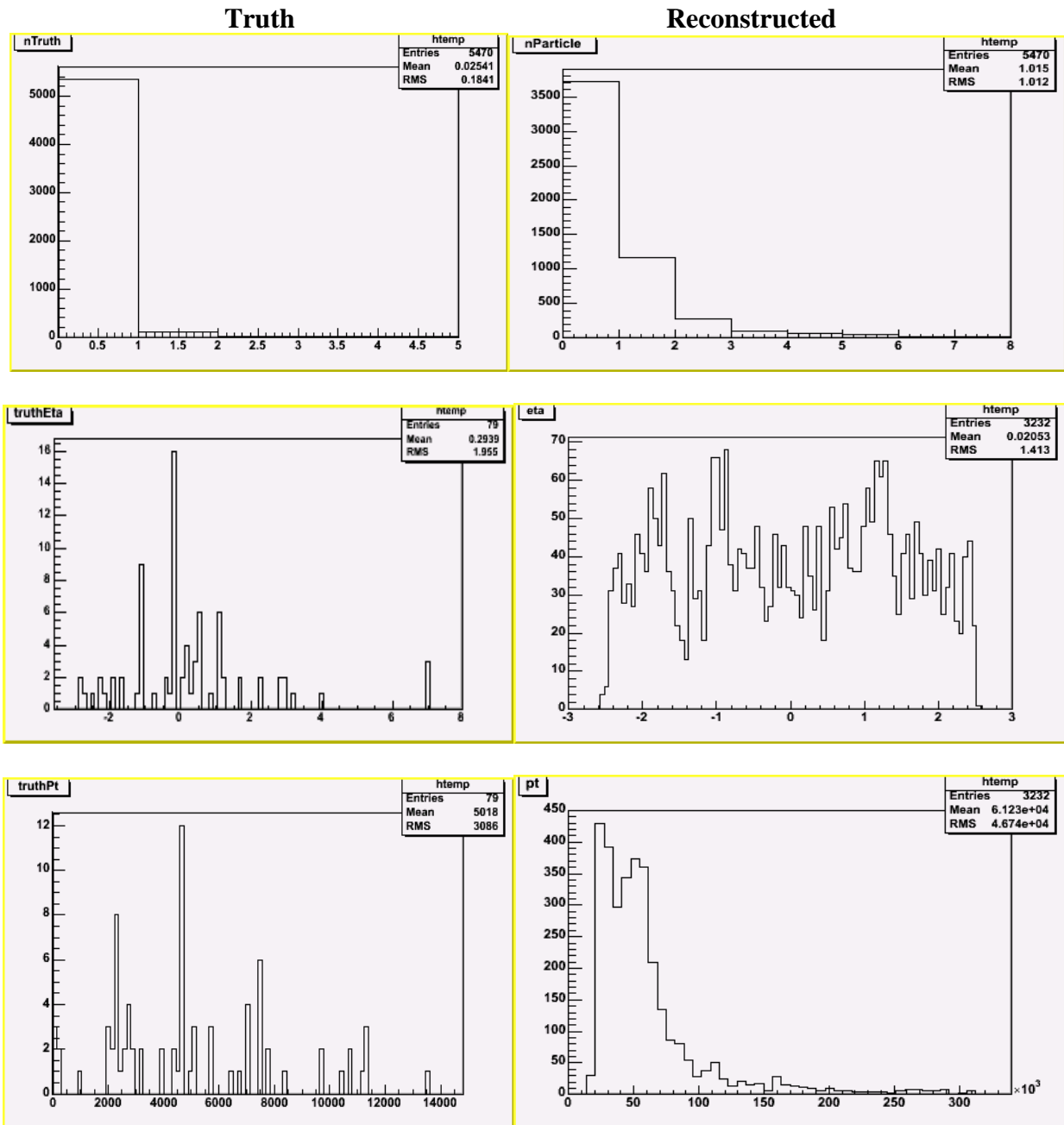


Figure 12 – Truth and reconstructed electron histograms

Particle Jets

Not many differences exist between the truth and reconstructed distributions for particle jets. Comparisons of the energies and transverse momenta between truth and reconstructed jets reveal very similar patterns. However, there are approximately 7,000 additional particle jets in the reconstructed data, possibly coming from photons and electrons being categorized as jets in the reconstruction. Also, notice the truth and reconstructed eta distributions. Truth particle jets are defined where $\eta \leq \pm 5.0$, but the detector can only identify particle jets where $\eta \leq \pm 4.75$. Other important differences are the dips in the reconstructed jet distribution at $\eta = \pm 1.5$ and $\eta = \pm 3.5$, which come from the detector's inefficiencies due to cracks between the barrel and end caps and the region where the end caps meet the forward calorimeter.

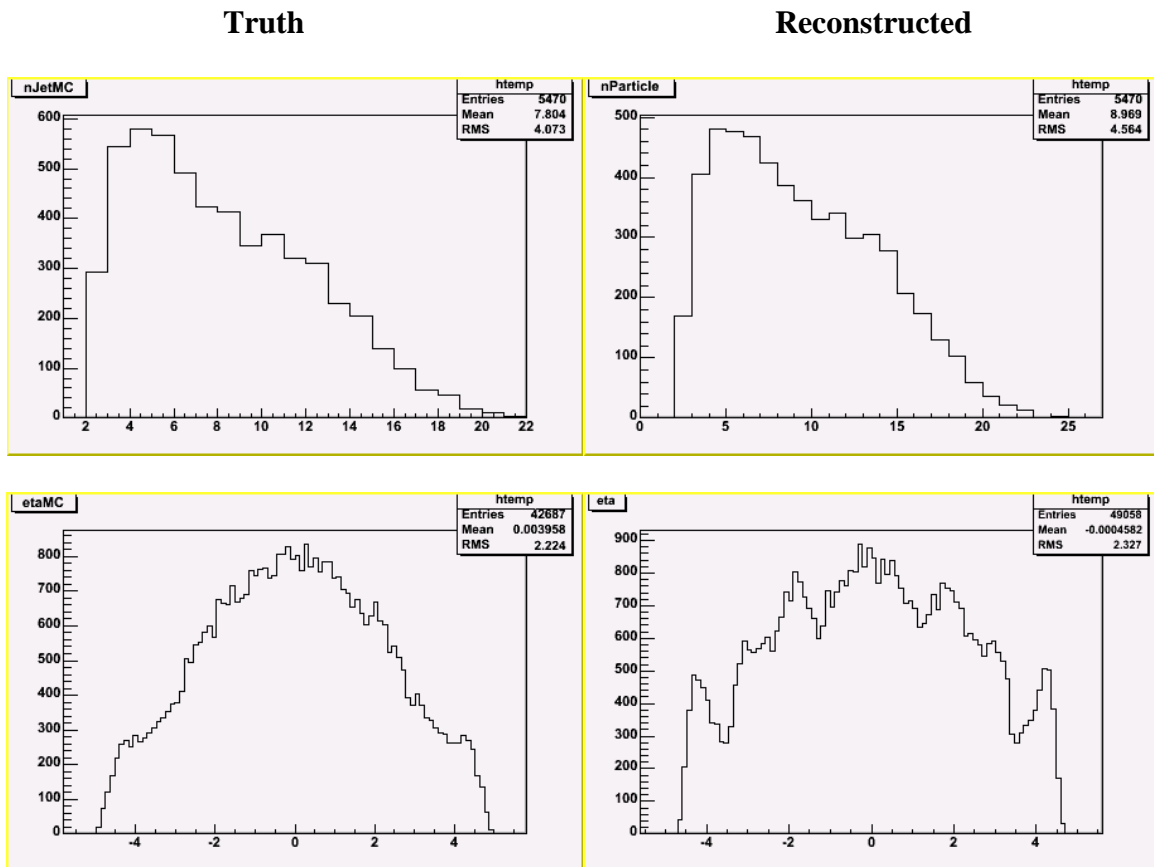


Figure 13 – Truth and reconstructed particle jet histograms

Truth

Reconstructed

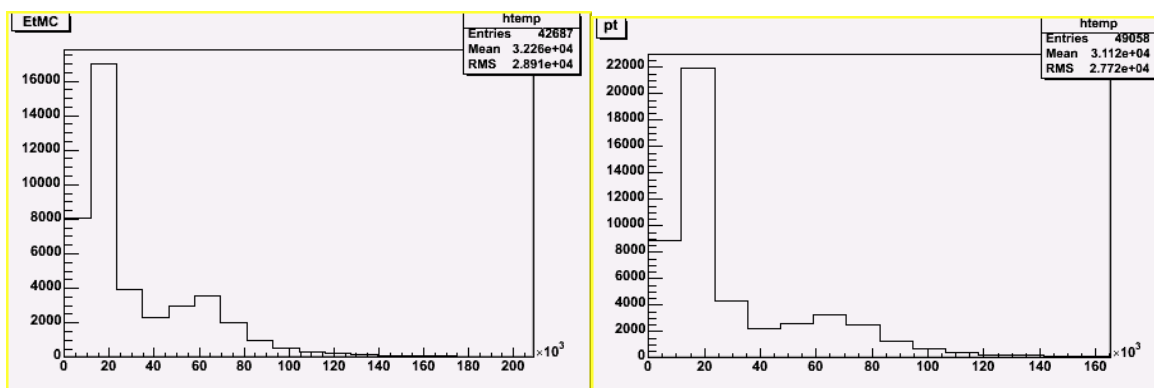


Figure 13 cont. – Truth and reconstructed particle jet histograms

Muons

There is a very large difference between the number of muons generated and the number of muons detected; roughly a 22,000 muon difference. This difference is due mostly to pions in particle jets that have decayed inside the detector into muons, and were not included by the Athena software into the truth particle container.

Truth

Reconstructed

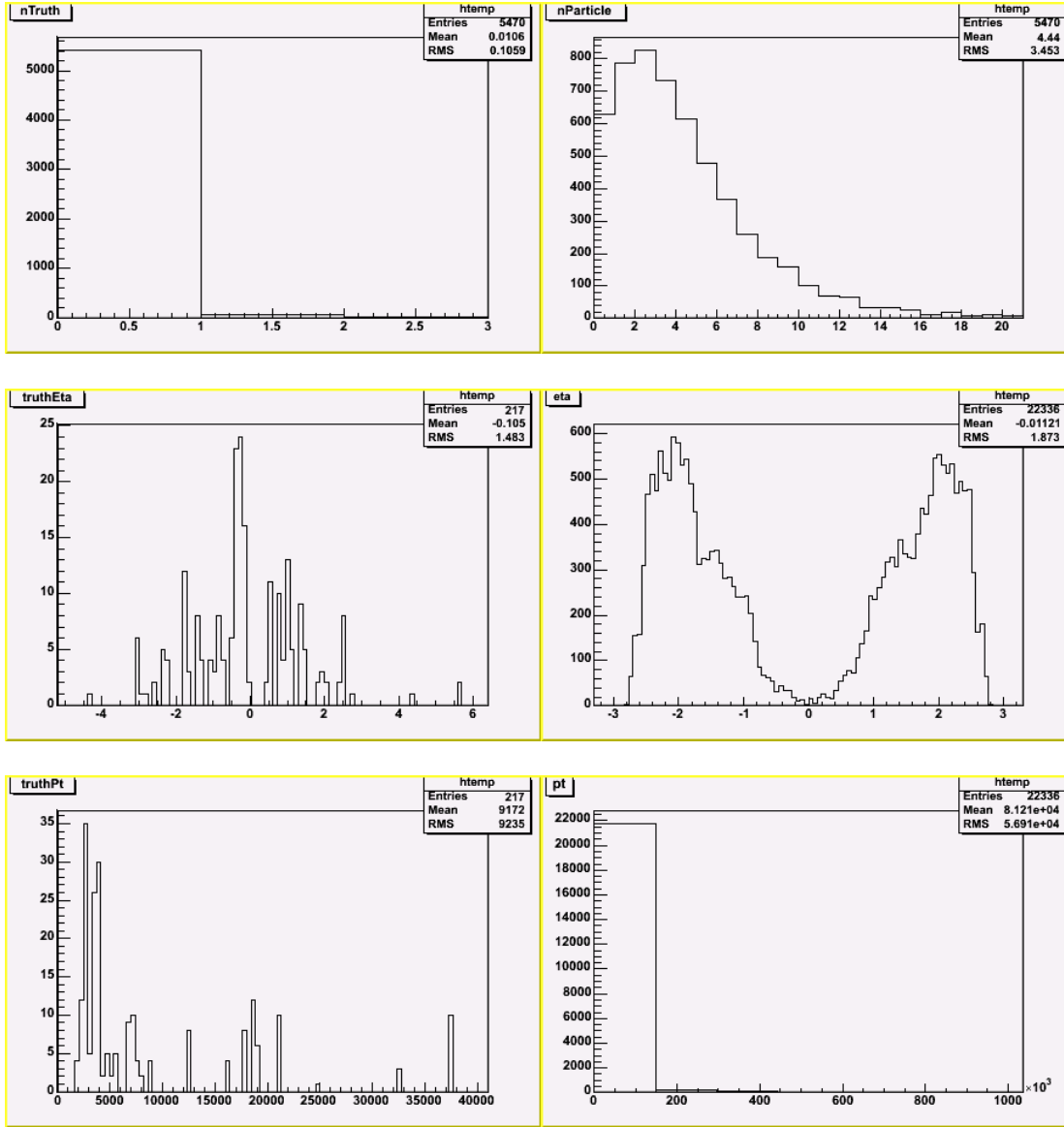
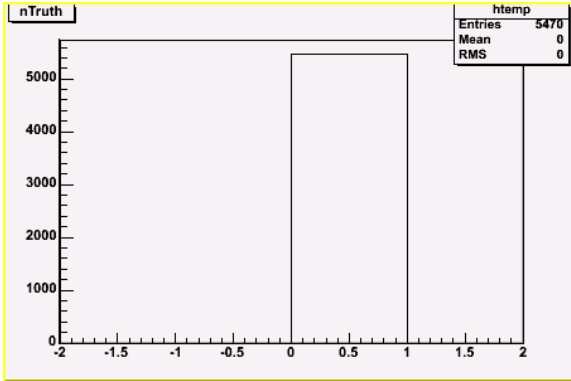


Figure 14 – Truth and reconstructed muon histograms

Tau Jets

There were absolutely no truth tau jets generated, and thus there are no truth eta and truth pt histograms. It is possible that many of the reconstructed tau jets are misidentified photons.

Truth



Reconstructed

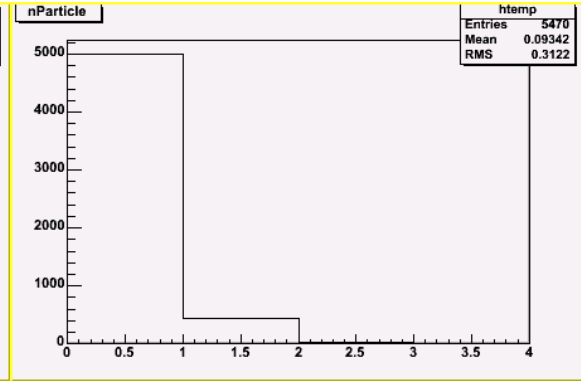
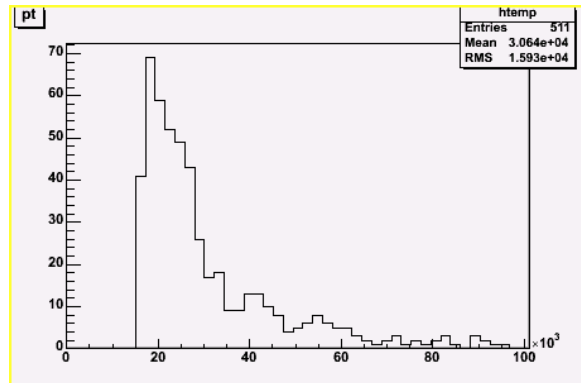
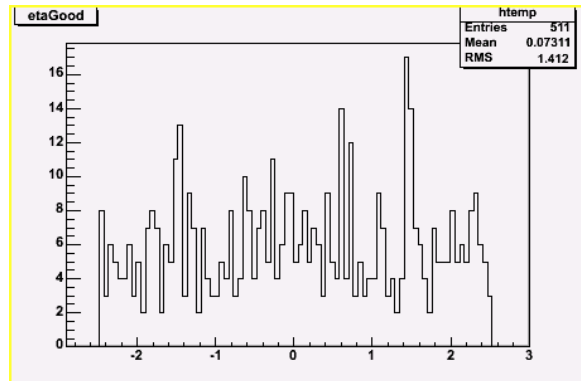


Figure 15 – Truth and reconstructed tau jet histograms



Missing Transverse Momentum

In every proton-proton collision, momentum must be conserved. In theory, every event must have the momenta of all the detected particles add up to zero in all three directions. But because particles may travel along the beam-axis without being detected,

in practice one can only add up the momenta in the two perpendicular, or x- and y- directions. After adding up the momenta in these directions, the amount that the sum differs from zero is known as the missing pt, and can be used to infer the existence of neutrinos, supersymmetric particles, or other particles which can take away momentum from the event without being seen in the detector.

In addition to analyzing the background particles, we also studied the missing pt for each event. The histograms below detail the total missing pt and its x- and y- components. The distributions of missing pt in the x- and y-directions display Gaussian distributions about zero with RMS values of approximately 10.6 GeV, and the total missing pt distribution shows a mean value of 12.2 GeV. As we would expect, the distribution of events with large missing pt diminishes above this mean. When ATLAS goes online in 2007, events which produce neutrinos, and possibly SUSY particles, may have signatures of large missing pt. However, there were no neutrinos or SUSY particles present in our simulation.

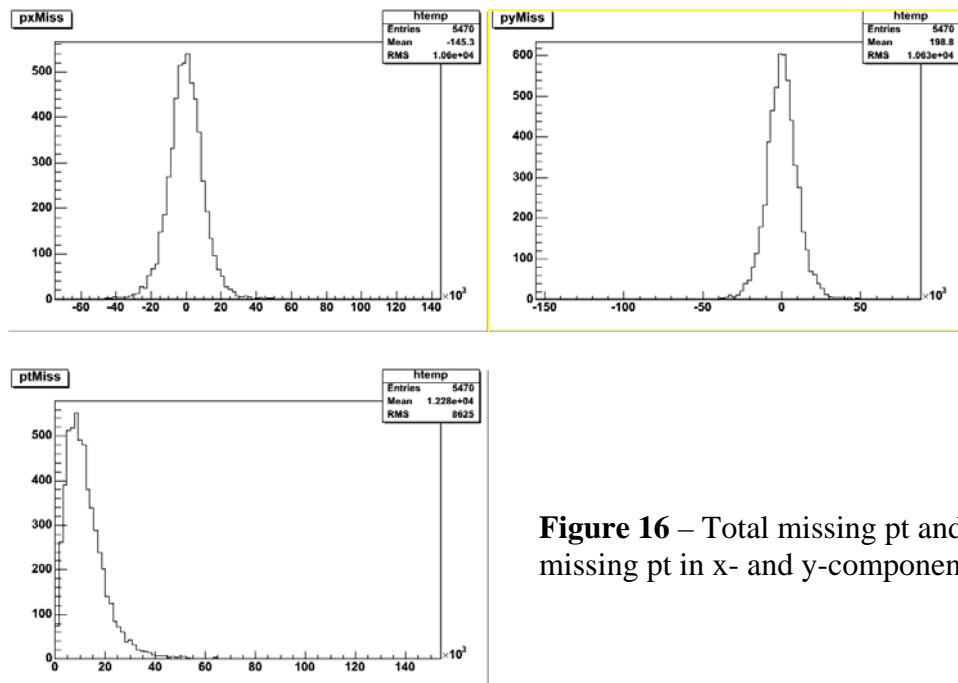


Figure 16 – Total missing pt and missing pt in x- and y-components

Mass of the Higgs Boson

In addition to studying the background particles produced in each event, we also examined the mass of the Higgs boson produced in the sample events. The condition placed on the generation of the events required that the Higgs boson decay into two photons. However, the reconstruction of each event yielded between one and six photons per event. To calculate the mass of the Higgs, we took all possible combinations of two photons for each event, and calculated the invariant mass of each combination. We then compared this invariant mass distribution with the distribution coming from events which had two and only two photons each with energy greater than 10 GeV. This tight selection of events eliminated any combinations of photons that were not a part of the Higgs decay. Although it may seem superfluous to measure the mass of a particle which was set at exactly 120 GeV when the events were generated, this method is useful because it shows the efficiency and resolution of the reconstruction program in measuring and recording energy values. The histogram in figure 16 displays the peak of the graph near 120 GeV, which is the expected mass of the Higgs boson.

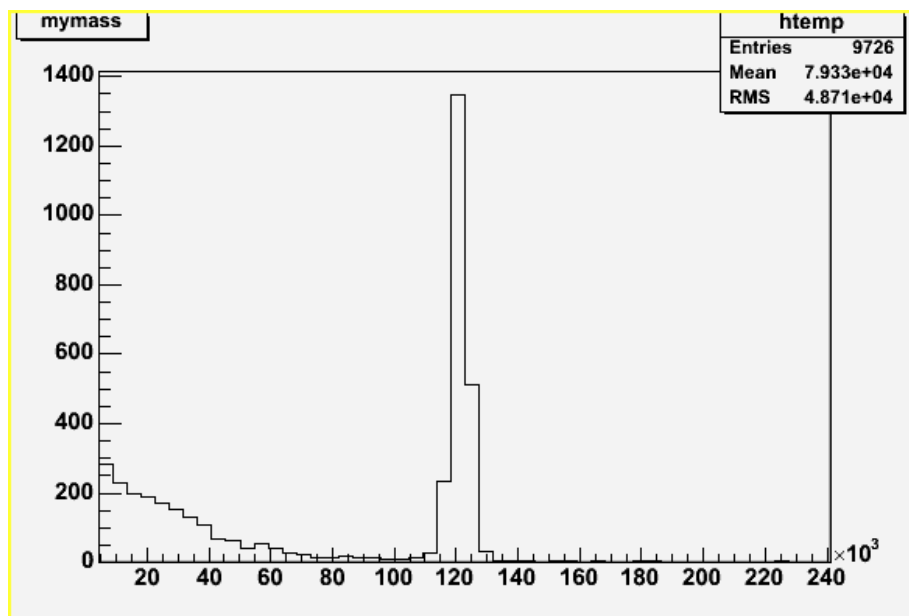


Figure 17 – Mass of the Higgs boson with all possible combinations of photons included

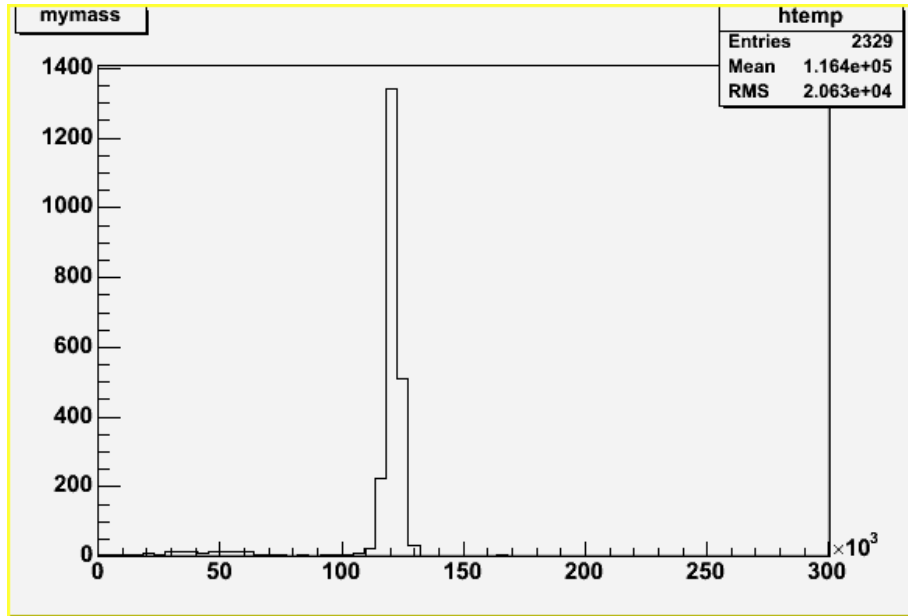


Figure 17 cont. – Mass of the Higgs boson after cuts

Total Energy of Particle Jets for Each Event

We also examined the total energy and transverse momentum of each event. We did this by adding the energies and transverse momenta of all the jets found in the particle jet class for each event. We used the particle jet class to look at total energy because all jets, including bjets and tau jets are included, as well as many of the photons and electrons which also pass the jet reconstruction algorithm.

The distribution of the total energy of the jets in each event had a mean of 1.55 TeV, which is slightly more than 10% of the total energy available in the collision. This tells us that, even considering energy from particles which did not get counted in the jets, or which may have passed through cracks in the detector, the majority of the total energy of the collision is not seen by the experiment. Much of this energy may be lost in the far forward direction, along the beam axis. The distribution of the total transverse momentum of the jets in each event had a mean of 300 GeV. The high ratio of total energy to total transverse momenta is reasonable given the large eta of many of the jets.

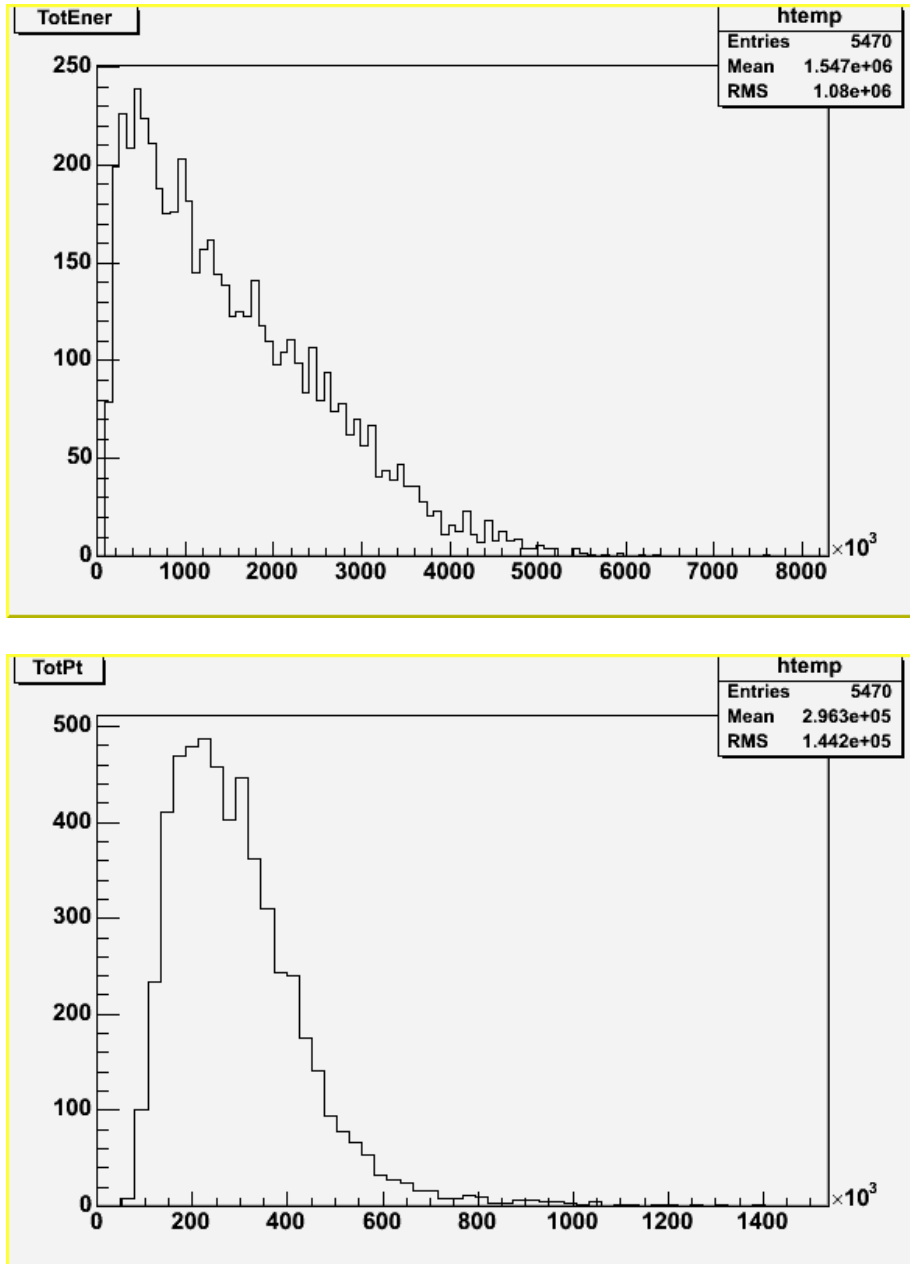


Figure 18 – Total energy and total transverse momentum of all particle jets in each event

Conclusion

The intentions of this project as initially set forth were achieved in that we now have an idea of the types of particles we can expect to see, and what their energy and angle distributions might look like, for each event when the ATLAS experiment goes online in 2007. Although we studied only one of the many possible Higgs boson decay

channels (where the Higgs decays into two photons), we may expect similar background results for any of the other decay channels.

In this project, we were able to observe the inefficiencies of the detector where the barrel calorimeters meet the end cap calorimeters, and where the end cap calorimeters meet the forward calorimeter. We were also able to determine that the reconstruction program, Athena, was misidentifying some photons as electrons, particle jets, and tau jets, leading us toward steps in debugging the reconstruction code. Finally, we were able to get an idea of the distribution of missing p_t that we can expect to see for particles that ATLAS is designed to identify. From this, we know the limits of the missing p_t we can realistically observe in our detector, and if missing p_t is found to be higher than this limit, we may be able to attribute that to neutrinos or supersymmetric particles. In concluding this project, we have begun to identify the types of things to look for when ATLAS goes online, and hopefully pointed the way to improvements which can be made to ensure that ATLAS is a success.

References

1. Atomos. Apr 10 2005.
<http://dbhs.wvusd.k12.ca.us/webdocs/AtomicStructure/Greeks.html>
2. Index of Particles. Apr 10 2005. <http://hyperphysics.phy-astr.gsu.edu/hbase/particles/>
3. Roe, Byron P. Particle Physics at the New Millennium. New York, New York: Springer-Verlag, 1996.
4. Cottingham, W.N. & D.A. Greenwood. An Introduction to the Standard Model of Particle Physics. Cambridge, UK: Cambridge University Press, 1998.
5. Serway, Raymond A., Clement J. Moses, & Curt A. Moyer. Modern Physics. USA: Thomson Learning, Inc., 1997
6. Perkins, Donald H. Introduction to High Energy Physics. Menlo Park, CA: Addison-Wesley Publishing Company, Inc., 1987.
7. Particle Physics Booklet. Extracted from the *Review of Particle Physics* K. Hagiwara *et al.*, Physical Review **D 66**, 010001 (2002).
8. ATLAS Experiment website. Apr 10 2005. <http://atlas.web.cern.ch/Atlas/>
9. ATLAS Collaboration, A.Airapetian et al.
The ATLAS detector physics performance Technical Design Report, Vol.I, ISBN 92-9083-141-3, 1999.